Progress In Electromagnetics Research, Vol. 106, 321–333, 2010

PLANAR UWB ANTENNA WITH 5 GHz BAND REJECTION SWITCHING FUNCTION AT GROUND PLANE

C.-Y.-D. Sim

Department of Electrical Engineering
Feng Chia University
Taichung 40724, Taiwan, R.O.C.

W.-T. Chung and C.-H. Lee

Department of Electronics Engineering
National Changhua University of Education
Changhua 500, Taiwan, R.O.C.

Abstract—The design of an octagonal-shaped microstrip-fed planar monopole antenna for ultrawideband (UWB) operation is studied. Two inverted T-shaped slits are embedded on the ground plane to allow band rejection characteristic from 5 to 6 GHz (for VSWR < 2). To enable switching capability for this band rejection function, a PIN diode is connected to each slit via a specified chip inductor that will be further investigated. Several prototypes were constructed and the measured results show that the proposed antenna can provide an operating bandwidth from 3.07 to 10.7 GHz, except for the rejected band. Simulation analyses are also carried out to validate the experimental results.

1. INTRODUCTION

Short-range indoor wireless communication devices with wideband operation are a promising technology for future applications such as modern electronics-healthcare system, wireless body area network (WBAN) and wireless personal area network (WPAN). Hence, a single antenna with wide enough bandwidth that will respond to multiple band of interest is desirable for such devices, and the approval for the unlicensed used of UWB application in 2002 has since open up

Received 2 June 2010, Accepted 30 June 2010, Scheduled 25 July 2010
Corresponding author: C.-Y.-D. Sim (cysim@fcu.edu.tw).

a new era in antenna design between 3.1 to 10.6 GHz. Thereafter, many different types of UWB antenna design with dissimilar sizes and shapes are proposed [1–9]. Among these designs, the microstrip-fed planar UWB antenna [9] has attracted significant attention due to its compactness, high data rate, satisfactory radiation properties, ease in fabrication, and low in manufacturing cost. For such design, its impedance matching is commonly achieved by tuning the gap distance between the patch and the ground plane.

Although the Federal Communications Commission (FCC) has imposed a strict broadcast power distribution on UWB, so that its emitting energy will not disrupt the existing applications such as wireless local-area network (WLAN) for IEEE 802.11a and HIPERLAN/2 operating in the 5.15 to 5.825 GHz band, a potential interference to these bands are still possible to exist if the UWB devices are within a close proximity. Therefore, a single band rejection function (or also known as band notch function) for UWB antenna designed with around 1 GHz depth from 5 to 6 GHz are extensively studied recently. Besides the conventional techniques to achieve band rejection by loading a single or multiple slot/slit onto the radiating element [10–12], other unusual methods such as placing two parasitic patches near the radiating element [13, 14], inserting a quarter-wavelength stub or dual stub within a slot [15, 16], and the embedding of a resonant cell or spur-line into the feeding-line are also reported [17–19]. From the aforementioned, novel techniques that will allow band rejection for UWB antenna have seems to be depleted, not until recently that a defected ground-plane structure (DGS) has been noticed once again, whereby the slot/slit from the radiating element are relocated to the ground plane [20–22]. By employing such method, it is interesting to realize that the average gain within the UWB is higher than the conventional techniques [22]. Furthermore, it is also noteworthy that even though a DGS such as slit loading the ground plane will excite a rejected band, a different slit loading approach or slight modification on the ground plane will also aids in improving the matching of the input impedance at the higher frequency range [16].

For the above mentioned designs, the rejected band is irreversible once the structure of the UWB antenna is fixed. Hence, an ON/OFF control using PIN-diode switches are proposed [23, 24], and if frequency agility for the rejected band is required, it can be achieved by replacing the PIN-diode by a varactor diode [25, 26]. Interestingly, the present open-literatures on band rejection switching are still rarely discussed, especially when the rejected band is excited from the ground plane instead of the radiating element. Furthermore, the effects of the chip inductor that are commonly used for RF isolation are not discussed

either [23], and the possibility of achieving agility for the rejected band using a varactor with a different value has also not been thoroughly studied.

Therefore, the design of an octagonal-shaped planar monopole antenna is initially studied [20]. By inserting two inverted T-shaped slit at both sides of the ground plane, a band rejection function at around 5 GHz is excited. In addition, its ability to perform band rejection switching is accomplished by simply replacing the two small patches located at each vertical sides of the ground plane by two PIN-diodes, thereby saving the trouble to create any additional narrow slits for DC block, which is a common practice presented in [23, 24]. Note that the effects of different chip inductor values used for RF isolation, and the possibility of achieving a tunable rejected band behavior by replacing the PIN-diodes with varactor diodes are also investigated. In addition, to ensure that the proposed antenna is applicable to any short-range or high data rate UWB antenna, the frequency domain characteristics are also measured and presented.

2. ANTENNA STRUCTURE

The geometry of the two octagonal-shaped prototype (A and B) monopole antennas with DGS is presented in Figure 1. Both prototype antennas are fabricated on a FR4 substrate of thickness 1.6 mm and permittivity 4.4. The dimensions of the microstrip feed line is 11 mm $\times$ 3 mm, and the radiating octagonal patch is with side length 6 mm and apothem 7.5 mm. To achieve optimum impedance matching at UWB, a 3 mm square slit is loaded at the middle of the ground plane as depicted in Figures 1(b) and (c). As for the proposed prototype A antenna, two inverted-T shaped slits are loaded at each upper end of the ground plane, so that a band rejection function can be achieved at around 5 GHz. For this case, three vital parameters should be considered, they are; dimension a (the horizontal length of the inverted-T slit), dimension b (the vertical length of the inverted-T slit), and dimension c (the distance away from the side of the ground plane). In order to perform band rejection switching capability, two small portions of ground plane located along dimension a are removed and replaced by two PIN-diodes (SC79) as depicted in Figure 1(c). Note that this unique design is able to avoid the extra effort to embed an additional DC block. As for the three chip inductors (JCI-2012C-27N) that are employed as RF isolation of the ground patch from the 3 volts DC battery source, two of the chip inductors are connected between the positive terminal of the source and the antenna's ground plane, while only a single chip inductor is linked between the negative terminal and

the ground plane. Note that the placing of these inductor chips is due to the excitation of the rejected band is from the two slits embedded

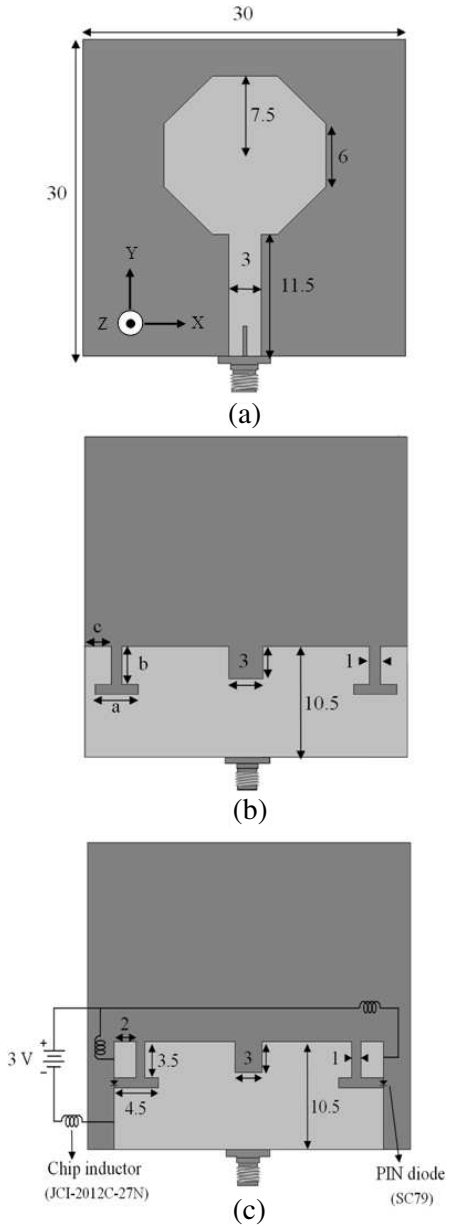

Figure 1. Geometry of the proposed ultrawideband antenna, (a) front, (b) back — Prototype A, and (c) back — Prototype B. (Units in mm).

in the ground plane.

3. UWB ANTENNA WITH BAND REJECTION FUNCTION (PROTOTYPE A)

The case when only both inverted T-shaped slits are loaded (Prototype A antenna) is first discussed. In this case, the 3 vital parameters, a, b, and c, are discussed in details for achieving the desired notched-band or depth. Figure 2 presents the measured return loss for various dimension a while both b and c are fixed at 3.5 and 2 mm, respectively. From this figure, it clearly shows that an increase or decrease in a will results in shifting of the rejected band to the lower or upper frequency band, respectively. In addition, when a is either 4.5 or 3.5 mm, a mismatch in impedance is observed at around 8 to 9 GHz band. As for the measured return loss depicted in Figure 3 for various dimension b while both a and c are fixed at 4 and 2 mm, respectively, it demonstrated a similar phenomena as in Figure 2 when b is increased or decreased, except that the shifting of the rejected band is more farther away with an increase in the notched depth. Here, it is also observed that if b is selected to be 4.5 mm or reduced to 2.5 mm, its lower-end operating frequency will be shifted higher to around 3.4 GHz, therefore unable to operate at UWB. Note that dimensions a and b (which form the inverted T-shaped slit) are responsible for the excitation of this rejected band which can be seen from the half wavelength current distribution plot presented in the next section. Therefore, the shifting of the rejection band can be achieved by simply tuning both parameters. In Figure 4, an increase in dimension c will

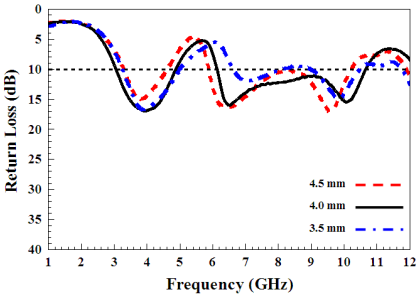

Figure 2. Measured return loss for the proposed prototype A with various dimension a while b = 3.5 mm, and c = 2 mm.

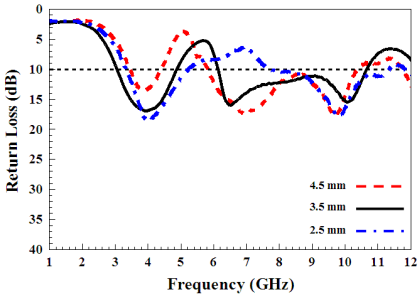

Figure 3. Measured return loss for the proposed prototype A with various dimension b while a = 4 mm, and c = 2 mm.

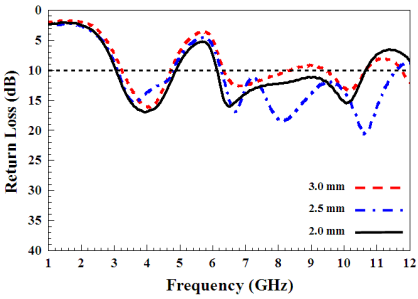

Figure 4. Measured return loss for the proposed prototype A with various dimension c while $a = 4\,\text{mm}$, and $b = 3.5\,\text{mm}$.

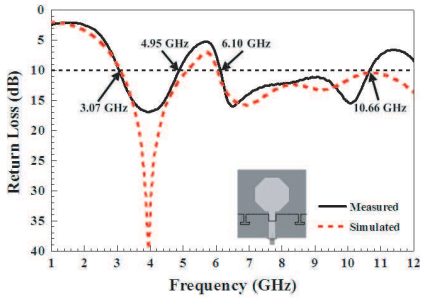

Figure 5. Measured and simulated return loss for the proposed prototype A.

only slightly enlarge the notched depth while the center of the notch frequency lingers around the origin. Furthermore, if c is increased up to 3 mm, an impedance mismatch will incur in the 8 to 10 GHz band. Therefore, to achieve a rejected band centered at around 5.5 GHz with a rejected bandwidth of around 1 GHz for prototype A antenna, the optimum dimensions for a, b, and c are set to be 4, 3.5 and 2 mm, respectively. Both the simulated and measured return loss of prototype A are presented in Figure 5 with good agreement. The rejected band for this case at along 10 dB return loss is measured between 4.95 to 6.1 GHz with a center frequency f_c calculated to be 5.525 GHz.

4. UWB ANTENNA WITH BAND REJECTION SWITCHING FUNCTION (PROTOTYPE B)

A novel method of modifying prototype A antenna to achieve a switching function on the rejected band is introduced in this section, and its photograph is shown in Figure 6. As aforementioned, by simply turning "ON" or "OFF" the 3 volts supply via the three chip inductors, the two loaded PIN-diodes on prototype antenna B will control the switching of the rejected band. Figure 7 presents the return loss results for the proposed prototype B antenna with switching function. With the 3 volts supply switched "OFF", which in turn will set both PIN-diodes at "OFF" states, the return loss in this case is similar to the original antenna without any T-shaped slits loaded (prototype C), demonstrating a common UWB antenna operating between 3.09 to 10.08 GHz. When the voltage supply is switched "ON", both PIN-diodes will be at "ON" state as well, and a rejected band measured

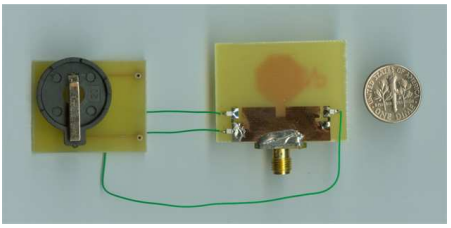

Figure 6. A photograph of prototype B antenna.

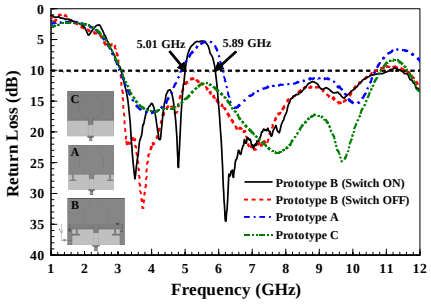

Figure 7. Measured return loss for the proposed prototype B with PIN-diodes switched "ON" or "OFF" in comparison to prototype A and C.

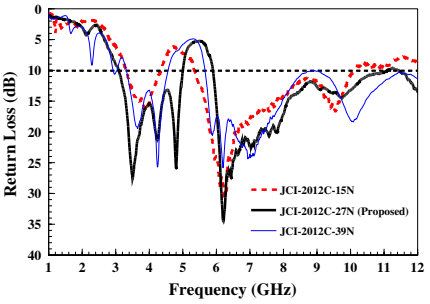

Figure 8. Measured results for prototype B loaded with different value of chip inductors for RF isolation when the supply/switch is at "ON" state.

from 5.01 to 5.89 GHz is presented. Although the depth of the rejected band (from 5.01 to 5.89 GHz) for prototype B is slightly narrower than prototype A, it is still within the rejected band of interest for IEEE 802.11a. Furthermore, a much better impedance matching at the lower and upper band is also observed besides the rejected one.

During the experimental measurement, it was realized that the value of the embedded chip inductors will also affect the performances of the UWB antenna, especially the rejected band. Note that due to limited resources, only 3 types of chip inductor (model: JCI-2012C) with different values of inductance at 15 nH, 27 nH (proposed), and 39 nH are available to the authors. Figure 8 presents the return loss of prototype B when different chip inductors are loaded with the voltage supply at "ON" state. In this figure, it is interesting to learn that a decrease or increase in chip inductance values for RF isolation will cause a shift in the rejected band to the lower frequency. This phenomenon could be related to the impedance excited by the rejected

band at 5.6 GHz, whereby the chip inductance at 27 nH is somehow matched to the rejected band. Notably, a slight shifting in the lower frequency band that moves beyond the required lower-end frequency (3.1 GHz) for UWB is also observed.

Figure 9 presents the peak gain variation for all prototype antennas. When the diodes are switched from "OFF" to "ON" state, the gain for prototype B is decreased sharply by 7 dB at the rejected band. Furthermore, prototype B has demonstrated a lower gain along the band of interest (except the rejected band) as compared to the prototype A, which could be due to the power dissipation in the diodes. Note that similar phenomenon is also observed for prototype C as well. To further validates that this drastic reduction in gain measured at 5.6 GHz is due to the two loaded slits, the simulated current distribution diagram of prototype B at the rejected band is presented in Figure 10. In this figure, a half-wavelength current distribution is observed along the inverted T-shaped slits, whereby this excited resonance is highly dependent on the dimensions a and b as presented in Figures 2 and 3, respectively. The measured radiation patterns of prototype B in the two principal planes at 4, 7 and 10 GHz are shown in Figure 11. A near omni-directional pattern is observed at the xz plane for 4 and 7 GHz. Note that Figure 11 is plotted when the switches are at "ON" states, and its patterns are almost identical when the switches are at "OFF" states. Hence, for brevity, only the "ON" states radiation patterns are plotted.

To obtain the frequency-domain characteristics, two identical prototypes B at "ON" state are placed in an Anechoic Chamber with co-polarized position (face to face), and the distance between them is

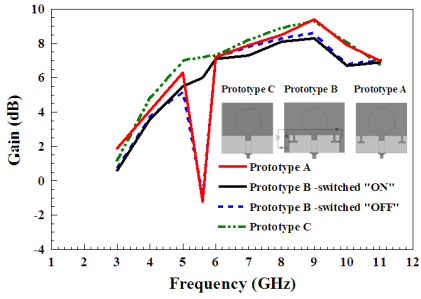

Figure 9. Peak gain variation for all prototypes antenna.

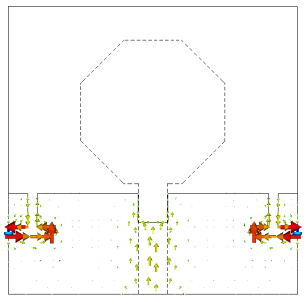

Figure 10. Current distribution of prototype B at the rejected band with Pin-diodes at "ON" state.

50 mm. The measured group delay in Figure 12 has demonstrated a delay of less than 1 ns within the UWB operation, except within the rejected band which shown a delay of more than 8 ns. It thus verified that the overall transmission performances of this proposed prototype B are adequate for any short-range UWB communication applications.

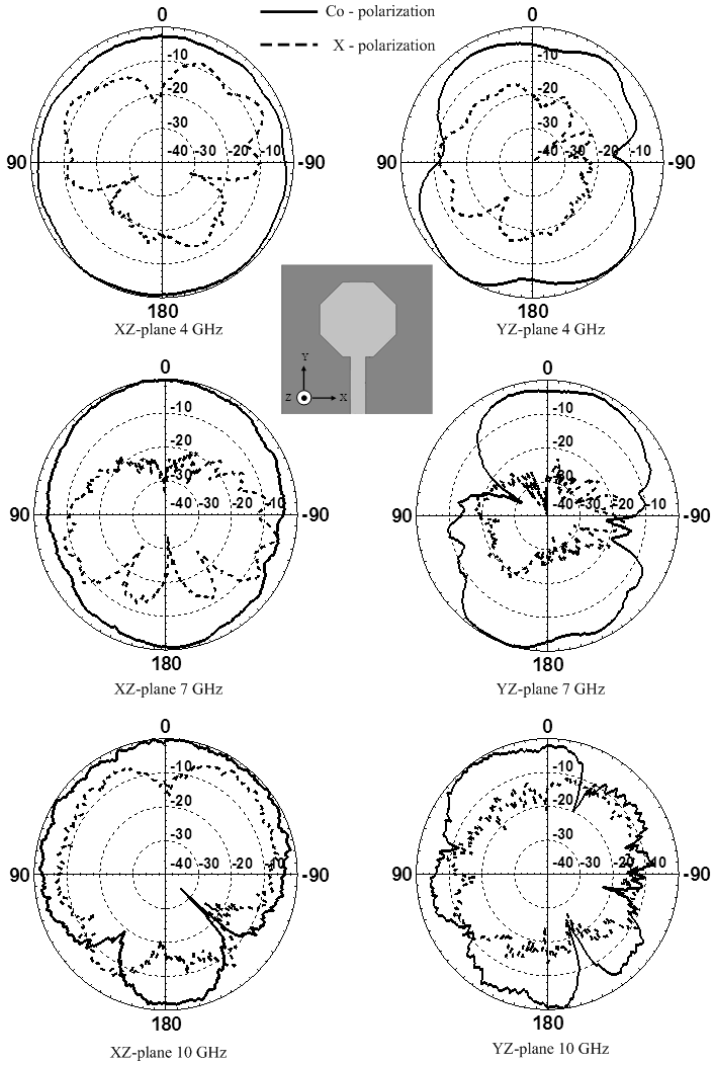

Figure 11. Measured radiation patterns of prototype B at 4, 7 and 10 GHz at "ON" states.

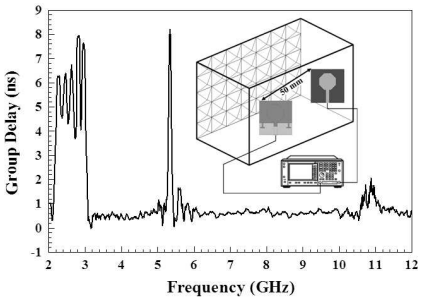

Figure 12. Group delay measurement of prototype B (face to face).

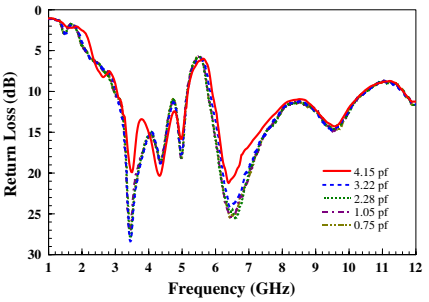

Figure 13. Return loss measurement for different capacitance values.

Lastly, during the investigation on prototype B, a question was raised if a tunable band rejection function can be achieved if the two loaded Pin-diodes are replaced by varactor diodes as studied in [25]. Hence, an experiment was conducted by employing two varactor diodes (model: SMV-1232) that will provide a variable capacitance values from 0.72 to 4.15 pF by tuning the voltage across it from 15 to 0 volts. From the results presented in Figure 13, the return loss at UWB are almost the same when the capacitance value is tuned from 0.72 to 3.22 pF, except a slight variation at the upper-end of the rejected band is observed at 3.22 pF. When the capacitance value is increased to 4.15 pF, the upper-end of the rejected band is increased from 5.89 to 6.2 GHz, while its lower end at around 5.01 GHz remains the same. Although this phenomenon is slightly different to [25], whereby a distinct variation is observed, this result provides yet another method to fine tune the bandwidth of the rejected band.

5. CONCLUSIONS

A microstrip-fed octagonal-shaped monopole antenna for UWB applications with a rejected band at around 5 to 6 GHz was successfully investigated. Furthermore, parametric studies have also been conducted to provide vital information on how the various parameters of the embedded slit can affect the frequency and depth of the rejected band. A switching function on the rejected band was successfully demonstrated when the PIN-diodes were loaded to the antenna, and it was interesting to realize that the inserted chip inductors for RF isolation will also affect the performances of the rejected band. Further studies from the frequency-domain characteristics have shown a stable transmission within the band of

interest, and hence the proposed antenna is in favor for any short-range UWB communication applications.

ACKNOWLEDGMENT

This work was supported by the Feng Chia Project No. 08C42292.

REFERENCES

1. Naghshvarian Jahromi, M., "Compact UWB bandnotch antenna with transmission-line-FED," *Progress In Electromagnetics Research B*, Vol. 3, 283–293, 2008.
2. Lin, C.-C. and H.-R. Chuang, "A 3–12 GHz UWB planar triangular monopole antenna with ridged ground-plane," *Progress In Electromagnetics Research*, Vol. 83, 307–321, 2008.
3. Khani, H. and P. Azmi, "Performance analysis of a high data rate UWB-DTR system in dense multipath channels," *Progress In Electromagnetics Research B*, Vol. 5, 119–131, 2008.
4. Khan, S. N., J. Hu, J. Xiong, and S. He, "Circular fractal monopole antenna for low VSWR UWB applications," *Progress In Electromagnetics Research Letters*, Vol. 1, 19–25, 2008.
5. Chen, Y. L., C. L. Ruan, and L. Peng, "A novel ultra-wideband bow-tie slot antenna in wireless communication systems," *Progress In Electromagnetics Research Letters*, Vol. 1, 101–108, 2008.
6. Rajabi, M., M. Mohammadirad, and N. Komjani, "Simulation of ultra wideband microstrip antenna using EPML-TLM," *Progress In Electromagnetics Research B*, Vol. 2, 115–124, 2008.
7. Abbaspour, M. and H. R. Hassani, "Wideband star-shaped microstrip patch antenna," *Progress In Electromagnetics Research Letters*, Vol. 1, 61–68, 2008.
8. Dehdasht-Heydari, R., H. R. Hassani, and A. R. Mallahzadeh, "Quad ridged horn antenna for UWB applications, " *Progress In Electromagnetics Research*, Vol. 79, 23–38, 2008.
9. Han, T.-Y., C.-Y.-D. Sim, and W.-C. Wu, "Planar multilateral disc monopole antenna with variable band-notch function for Bluetooth/UWB applications," *Journal of Electromagnetic Waves and Applications*, Vol. 23, No. 17–18, 2289–2299, Dec. 2009.
10. Fallahi, R., A. A. Kalteh, and M. G. Roozbahani, "A novel UWB elliptical slot antenna with band-notched characteristics," *Progress In Electromagnetics Research*, Vol. 82, 127–136, 2008.
11. Lee, W. S., D. Z. Kim, K. J. Kim, and J. W. Yu,

"Wideband planar monopole antennas with dual band-notched characteristics," *IEEE Trans. Microwave Theory Tech.*, Vol. 54, 2800–2806, 2006.

12. Lin, Y. C. and K. J. Hung, "Compact ultrawideband rectangular aperture antenna and band-notched designs," *IEEE Trans. Antennas Propagat.*, Vol. 54, 3075–3081, 2006.
13. Kim, K. H., Y. J. Cho, S. H. Hwang, and S. O. Park, "Band-notched UWB planar monopole antenna with two parasitic patches," *Electron. Lett.*, Vol. 41, 783–785, 2005.
14. Lee, S. H., J. W. Bail, and Y. S. Kim, "A coplanar waveguide fed monopole ultra-wideband antenna having band-notched frequency function by two folded-striplines," *Microwave Opt. Technol. Lett.*, Vol. 49, 2747–2750, 2006.
15. Luo, C. H., C. M. Lee, W. S. Chen, C. H. Tu, and Y. Z. Juang, "Dual band-notched monopole antenna with an annular CPW-feeding structure," *Microwave Opt. Technol. Lett.*, Vol. 49, 2376–2379, 2007.
16. Hong, C. Y., C. W. Ling, I. Y. Tarn, and S. J. Chung, "Design of a planar ultrawideband antenna with a new band-notch structure," *IEEE Antennas Wireless Propag. Lett.*, Vol. 55, 3391–3397, 2007.
17. Qu, S. W., J. L. Li, and Q. Xue, "A band-notched ultrawideband printed monopole antenna," *IEEE Antennas Wireless Propag. Lett.*, Vol. 5, 495–498, 2006.
18. Ding, Y., G. M. Wang, and J. G. Liang, "Compact band-notched ultra-wideband printed antenna," *Microwave Opt. Technol. Lett.*, Vol. 49, 2686–2689, 2007.
19. Abbosh, A. M., "Ultra wideband planar antenna with spurline for subband rejection," *Microwave Opt. Technol. Lett.*, Vol. 50, 725–728, 2008.
20. Sim, C.-Y.-D., W.-T. Chung, and C.-H. Lee, "Printed UWB monopole antenna embedded with L-shaped slots in the ground plane for 5 GHz band-notch function", *Journal of Electromagnetic Waves and Applications*, Vol. 22, No. 14–15, 1965–1974, Dec. 2008.
21. Sim, C. Y. D., W. T. Chung, and C. H. Lee, "An octagonal UWB monopole antenna with 5 GHz band-notch function," *Microwave Opt. Technol. Lett.*, Vol. 51, 74–78, 2009.
22. Sim, C. Y. D., W. T. Chung, and C. H. Lee, "A circular-disc monopole antenna with band-rejection function for ultrawideband application," *Microwave Opt. Technol. Lett.*, Vol. 51, 1607–1613, 2009.

23. Shameena, V. A., M. N. Suma, K. Raj Rohith, P. C. Bybi, and P. Mohanan, "Compact ultra-wideband planar serrated antenna with notch band ON/OFF control," *Electron. Lett.*, Vol. 42, 1323–1324, 2006.
24. Yoon, S. W., L. H. Truong, H. S. Lee, E. J. Park, H. M. Park, J. K. Rhee, and H. C. Park, "UWB antenna with frequency diversity characteristics using PIN-diode switches," *ICACT 11th Int. Conf. Advanced Comm. Technol.*, 344–346, 2009.
25. Antonino, E., M. Cabedo, M. Ferando, and M. Baquero, "Novel UWB antennas with switchable and tunable band-notch behavior," *Proc. IEEE Int. Symp. Antennas Propag.*, 693–696, 2007.
26. Antonino, E., M. Cabedo, M. Ferando, and M. Baquero, "Compact ultra-wideband planar serrated antenna with notch band ON/OFF control," *Electron. Lett.*, Vol. 42, 1323–1324, 2006.